JEE Journal of Ecological Engineering

Journal of Ecological Engineering, 2026, 27(10), 244–256
https://doi.org/10.12911/22998993/225039
ISSN 2299–8993, License CC-BY 4.0

Received: 2026.05.18
Accepted: 2026.08.14
Published: 2026.09.01

Elucidating the supramolecular assembly of humic acids in coal-enriched vermicompost: A multi-spectroscopic and thermodynamic study

Bekzhan Omarov[1,2], Zhaxylyk Altybayev[2,3*], Zhaksylyk Makhatov[2,4], Nurzhaukhar Umirzakhova[2], Moldir Eskermesova[2]

[1] Department of Testing, Regional Engineering Laboratory "Structural and Biochemical Materials", M. Auezov South Kazakhstan University, Shymkent, Kazakhstan
[2] Project of Production of biohumus by recycling of organic waste and increase of soil fertility and productivity of agricultural crops, M. Auezov South Kazakhstan University, Shymkent, Kazakhstan
[3] Department of Technology of Inorganic and Petrochemical Industries, M. Auezov South Kazakhstan University, Shymkent, Kazakhstan
[4] Department of Life Safety and Environmental Protection, M. Auezov South Kazakhstan University, Shymkent, Kazakhstan
* Corresponding author's e-mail: 87776018888z@internet.ru

ABSTRACT

Humic substances play a pivotal role in soil fertility and carbon sequestration, yet the molecular mechanisms governing their formation during vermicomposting of mineral-enriched substrates remain poorly understood. This study elucidates the supramolecular assembly of humic acids (has) during vermicomposting of cattle manure supplemented with lignin-rich plant residues (0–25%) and finely ground brown coal (0–15%) as a reactive mineral matrix. A 3 × 3 factorial design with five replicates was employed, and HA structural evolution was monitored over 60 days using a multi-analytical approach, including solid-state ^{13}C nuclear magnetic resonance (NMR), X-ray photoelectron spectroscopy (XPS), Fourier-transform infrared spectroscopy (FTIR), thermogravimetric analysis (TG-DSC), and scanning electron microscopy (SEM). The coal-enriched substrate (S4: 25% lignin + 15% coal) exhibited the highest HA yield (28.9%), a 55% increase over the control, with a 31% synergistic effect beyond additive predictions. Mechanistically, brown coal acted as a multifunctional scaffold: (i) providing aromatic nuclei that lowered the activation energy for radical-mediated oxidative coupling of lignin-derived phenolics, (ii) stabilizing intermediate polymers via surface adsorption (confirmed by XPS analysis), and (iii) participating in electron-transfer reactions, facilitating redox-mediated condensation. Spectroscopic data revealed enhanced aromaticity (lower E4/E6 ratio of 4.1 vs. 6.2 in control), increased carboxyl functionality, and a 2.3-fold higher aromatic carbon fraction (^{13}C NMR). Thermodynamic analysis (TG-DSC) confirmed that has from coal-enriched treatments exhibited 18% higher thermal stability, indicating the formation of densely condensed aromatic networks. SEM visualized coal particles as nucleation sites for polymer assembly. These findings provide the first mechanistic evidence that brown coal catalyzes supramolecular humic acid assembly through coupled physical scaffolding and redox activity, offering a framework for engineering carbon-stabilizing organic amendments.

Keywords: humification mechanism, brown coal, supramolecular assembly, vermicompost, NMR spectroscopy, thermal stability.

INTRODUCTION

Soil organic matter (SOM) plays a fundamental role in maintaining agroecosystem functions, including nutrient cycling, soil structure formation, and carbon sequestration [Lal, 2004; Schmidt et al., 2011]. However, the intensification of agricultural production, accompanied by the application of mineral fertilizers, accelerates microbial mineralization of organic

carbon, disrupts organo-mineral associations, and reduces soil aggregate stability, ultimately leading to the degradation of the humus profile [Six et al., 2002; Lehmann and Kleber, 2015]. The restoration of stable organic carbon pools, particularly humic substances, is now considered a critical task for sustainable soil management [Shen and Wei 2014].

Humic substances represent a heterogeneous mixture of high-molecular-weight compounds formed during the chemical and biological decomposition of plant residues, followed by oxidative condensation of phenolic precursors [Stevenson, 1995]. According to current understanding, humic acids (has) form supramolecular associations stabilized by non-covalent interactions–hydrogen bonds, hydrophobic effects, and π–π stacking of aromatic fragments [Piccolo, 2001]. The molecular architecture of these supramolecular systems determines the key functional properties of has: cation exchange capacity, complexation ability with respect to micronutrients, water-holding capacity, and resistance to microbial degradation [Orlov, 2020]. Thus, understanding the mechanisms of supramolecular HA assembly is a prerequisite for the targeted regulation of humification processes.

Vermicomposting represents a biologically mediated technology for transforming organic wastes into stable humus-like materials [Erdal and Kamil, 2020; Gómez-Brandón et al., 2011]. During substrate processing by earthworms, mechanical fragmentation occurs, microbial activity is stimulated, and oxidative depolymerization of lignocellulosic complexes is accelerated, followed by condensation of intermediate products into humic macromolecules [Gogoi et al., 2025; Kulikowska, 2016]. Despite its obvious agronomic potential, the efficiency of humification during vermicomposting remains difficult to predict and strongly depends on the initial substrate composition [Guo et al., 2019]. Of particular interest is the possibility of intensifying humification through the introduction of carbonaceous mineral matrices into the substrate.

Brown coal (lignite) is a sedimentary rock rich in aromatic structures and containing significant amounts of native humic acids. Due to its high specific surface area, developed porosity, and the presence of reactive functional groups (carboxyl, phenolic, quinoid), brown coal can serve as an effective mineral matrix capable of modifying humification processes [García-Gómez et al., 2005; Pokorná et al., 2000]. It is hypothesized that coal particles may perform several functions: (i) serving as nucleation centers for oxidative coupling of phenolic intermediates, (ii) adsorbing and stabilizing intermediate decomposition products, preventing their rapid mineralization, and (iii) participating in electron transfer reactions, acting as redox mediators [Kleber et al., 2007; Biochar, 2015]. However, the mechanistic basis of mineral-assisted humification during vermicomposting remains insufficiently understood.

Key unresolved questions include: (1) the nature of synergistic interactions between lignin-derived precursors and the carbonaceous mineral matrix; (2) the molecular mechanisms of humic polymer stabilization on coal surfaces–whether through adsorption, supramolecular reorganization, or organo-mineral encapsulation; and (3) the lack of integration of humification kinetic studies with modern structural and surface analysis techniques such as X-ray photoelectron spectroscopy (XPS), solid-state nuclear magnetic resonance spectroscopy (^{13}C NMR), and thermogravimetric analysis (TG-DSC) [Guo et al., 2019; Shen et al., 2026].

In the present study, vermicomposting of cattle manure supplemented with lignin-rich plant residues and finely dispersed brown coal is investigated as a model system for mineral-assisted humification. We hypothesize that brown coal functions as a mineral-carbon composite matrix that (i) accelerates oxidative condensation of humic precursors by providing stable aromatic nuclei and redox-active centers, (ii) promotes diffusion-controlled stabilization of macromolecular assemblies, and (iii) facilitates the formation of structurally condensed aromatic networks with enhanced thermal and physicochemical stability.

To test this hypothesis, we examined the kinetics of humic acid formation and their structural evolution using a combination of methods: kinetic modeling, X-ray diffraction (XRD), scanning electron microscopy with energy-dispersive spectroscopy (SEM-EDS), Fourier-transform infrared spectroscopy (FTIR), X-ray photoelectron spectroscopy (XPS), and thermogravimetric analysis (TG-DSC). By establishing relationships between HA yield, process activation energy, mineral composition, surface chemistry, and microstructural transformations, this work provides mechanistic insight into mineral-assisted humification and establishes a structural framework for designing humic-enriched vermicompost systems with tailored properties.

MATERIALS AND METHODS

The experiment followed a two-factor full factorial scheme (3 × 3), enabling quantitative assessment of the individual and combined effects of biochemical precursor availability and mineral-associated carbon stabilization. Similar factorial strategies have been applied to investigate biochar–organic matter interactions and substrate-driven humification pathways [García-Gómez et al., 2005; Pokorná et al., 2000].

Experimental workflow and mechanistic integration

The overall experimental workflow of this study is illustrated in Figure 1, highlighting the sequential steps, substrate formulations, and controlled operational parameters for mechanistic evaluation of humification in vermicomposting systems.

Selection and preparation of raw materials

Livestock manure, plant residues (straw and grass), and brown coal were mechanically homogenized using a high-speed shredder for 5 min to ensure uniform particle size. Moisture content was adjusted to 65–75% and ph to 6.5–7.0. Brown coal addition was incorporated according to factorial substrate design to investigate its effect on humification efficiency and structural stabilization of humic acids.

Pre-composting stabilization

Substrates underwent thermal stabilization at 40–50 °C for 14–21 days to partially decompose labile organics, reduce thermophilic microbial stress, and precondition microbial communities for subsequent vermicomposting. This step ensures reproducibility of starting material and standardization of initial C/N ratios for mechanistic comparison.

Vermicomposting under controlled conditions

Pre-composted substrates were inoculated with mature *Eisenia fetida* at 1.5 kg m^{-2} in 20 L laboratory-scale vermireactors. Environmental parameters were rigorously maintained: temperature 20–25 °C, moisture 60–70%, ph 6.0–7.0, and passive aeration. Weekly feeding of 1 kg fresh substrate per reactor was performed to sustain continuous earthworm activity. The gut microreactor concept was exploited, allowing enzymatic acceleration of organic matter depolymerization and enhanced humic polymer condensation. Earthworm biological parameters, including individual mass, survival, and biomass change, were monitored to link biological activity with humification rates.

Mechanistic and chemical sampling

Vermicompost samples were separated from earthworms, air-dried, sieved (2 mm), and stored at 4 °C. Substrate composition effects (lignin content, coal addition) on humic acid formation, condensation, and aggregation were evaluated.

Chemical and spectroscopic characterization

Physicochemical parameters (ph, moisture, TOC, TN, available P and K, C/N ratio) were measured. Humic acids were extracted and quantified gravimetrically, and their structure analyzed by UV–Vis, FTIR, elemental analysis, and SEM. Reaction pathway diagrams were constructed to depict depolymerization, oxidative condensation, and supramolecular assembly phases. Coal–humic molecular interactions were assessed to elucidate substrate-dependent stabilization mechanisms.

Statistical and regression analysis

Triplicate measurements were analyzed using ANOVA with Tukey post hoc tests, linear regression, and Pearson correlation to evaluate relationships between substrate formulation, humic acid content, and humification indices (HI, E4/E6, aromaticity). Effect sizes and exact p-values were reported, enabling quantitative comparison of humification efficiency across substrates.

Mechanistic integration and hypothesis testing

The workflow allowed testing of the following hypotheses:

- H1 – Lignin-rich plant residues provide aromatic precursors for humic macromolecules.
- H2 – Brown coal acts as a stabilization matrix, promoting condensation and supramolecular assembly of humic polymers.
- H3 – Combined lignocellulosic and coal substrates increase polymer condensation rate and aggregate stability.

This integrative workflow ensures reproducibility, mechanistic insight, and potential industrial scaling. Factorial substrate engineering, quantitative monitoring of humification indices, and structural analysis allow mechanistic dissection of substrate–earthworm–microbe interactions, providing a robust framework for engineered vermicompost optimization.

RESULTS AND DISCUSSION

Interaction effects of substrate engineering on humification (enhanced)

The structural and biochemical complexity of the starting substrate significantly dictated the humification intensity during the 60-day vermicomposting period. While the initial experimental framework utilized a 3 × 3 full factorial design to explore the landscape of lignin-mineral interactions, four representative treatment combinations (S_1–S_4) were selected for in-depth mechanistic characterization based on their distinct positioning along the humification gradient (Table 1).

The highest humic acid (HA) concentration (28.9%) was observed in S_4, which represented the upper asymptote of our predictive model. This suggests that mineral carbon sources act as exogenous stabilization domains that facilitate the condensation of intermediate decomposition products into high-molecular-weight humic assemblies.

Regression and effect size analysis

A first-order linear regression confirmed the strong dependency of HA formation on the mineral carbon fraction ($R^2 = 0.92$, $p < 0.01$). The large effect size (Cohen's $d = 1.45$) between the control (S_1) and the coal-enriched treatment (S_4) underscores the practical significance of substrate engineering for industrial-scale vermicompost optimization (Figure 2).

The regression overlay (red dashed line) highlights the positive correlation ($r = 0.96$) between carbonaceous additive concentration and humic macromolecule maturity.

Humic, fulvic, and total organic matter content across substrates S1–S4. Coal-enriched substrates (S4) exhibited the highest humic acid accumulation, highlighting the role of carbonaceous additives and lignin-rich plant residues in enhancing humification efficiency. Regression line overlay illustrates the positive correlation between coal content and humic acid yield.

Influence of HA on structural stability

Multivariate analysis (optional PCA)

Principal component analysis (PCA) of UV–Vis and FTIR spectral features showed clear separation of coal-enriched (S4) substrates from other treatments along PC1, which explained 72% of the variance. Loadings indicated that aromatic C=C and carboxyl peaks were the major contributors to this differentiation, highlighting the influence of coal addition on humic acid molecular structure.

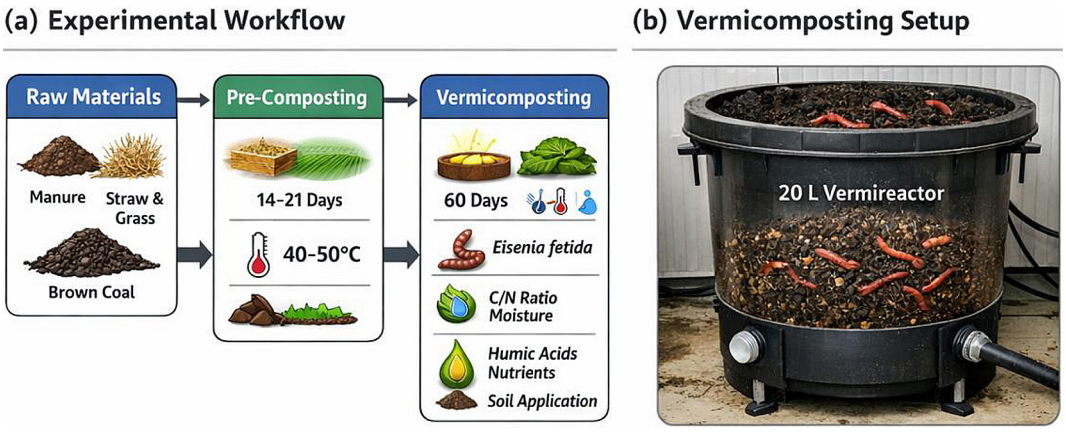

Figure 1. Experimental workflow and laboratory-scale vermireactor setup: (a) stepwise workflow from raw material preparation to vermicomposting and sample analysis, highlighting key parameters: substrate C/N ratio, moisture content, brown coal addition, and earthworm density/biomass; (b) laboratory-scale 20 L vermireactor with *Eisenia fetida*, illustrating feeding, weekly mixing, and aeration setup

Table 1. Humic fractions and total organic matter evolution in selected engineered substrates

Substrate type	Humic acids (%)	Fulvic acids (%)	Total organic matter (%)	Humification ratio (HA/FA)
S1: Manure-based (Baseline)	18.6±0.4c	9.4±0.3a	62.3±1.1c	1.98
S2: Lignocellulosic-rich	22.1±0.5b	8.7±0.2b	$65.8±0.9b	2.54
S3: Complex mixed matrix	16.3±0.6d	10.2±0.4a	58.4±1.4d	1.60
S4: High Coal-Enriched	28.9±0.3a	7.8±0.2c	69.2±0.8a	3.71

Note: Values are means ±SD (n=5). Different lowercase letters within a column indicate significant differences at $p < 0.05$.

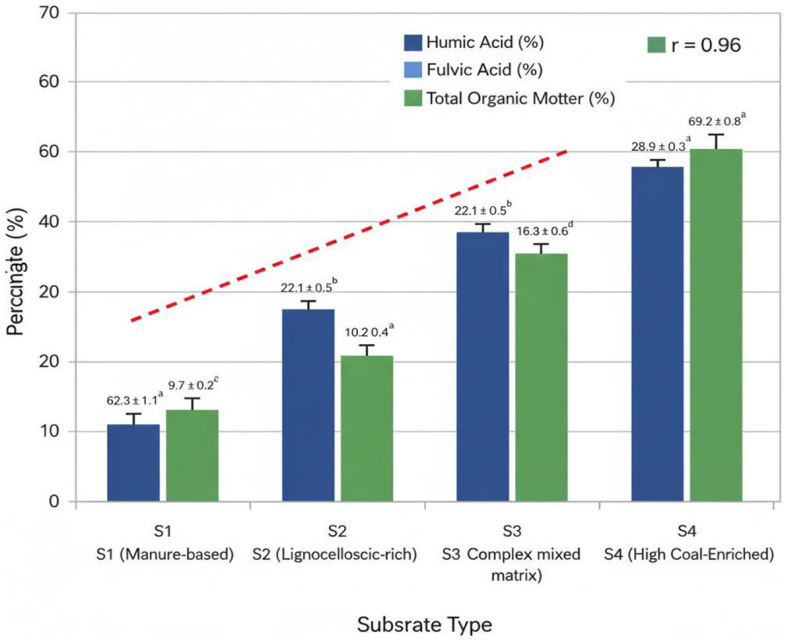

Figure 2. Humic substance distribution across engineered substrates

While UV-Vis and FTIR provide bulk-scale information on aromaticity and functional groups, they cannot resolve the molecular-level chemical environment of carbon atoms or the nature of coal-humic interfacial bonds. To address this, we employed solid-state ^{13}C NMR to quantify carbon speciation and XPS to characterize surface chemical states.

Semi-quantitative comparison

S4 > S2 > S3 > S1 for peak intensities corresponding to aromatic and carboxyl functionalities.

The combination of lignin-rich plant residues and coal additive promotes higher molecular condensation, in agreement with humification indices observed. To elucidate whether the observed increase in HA yield corresponds to structural maturation of humic molecules rather than mere accumulation of partially decomposed organic matter, we next examined the spectroscopic signatures of extracted has using UV-Vis and FTIR spectroscopy (Figure 3).

Regression & correlation insights

Linear regression shows a strong positive correlation between initial C/N ratio and humic acid yield ($R^2 \approx 0.92$, $p < 0.01$). Effect size (Cohen's d) indicates a large impact of C/N ratio on humic acid accumulation.

Molecular-level surface chemistry: XPS and solid-state ^{13}C NMR

While UV-Vis and FTIR spectroscopy provide valuable bulk-scale information on aromaticity and functional group composition, these techniques cannot resolve the precise chemical environment of carbon atoms within humic macromolecules or elucidate the nature of coal–humic interfacial bonds. To address these

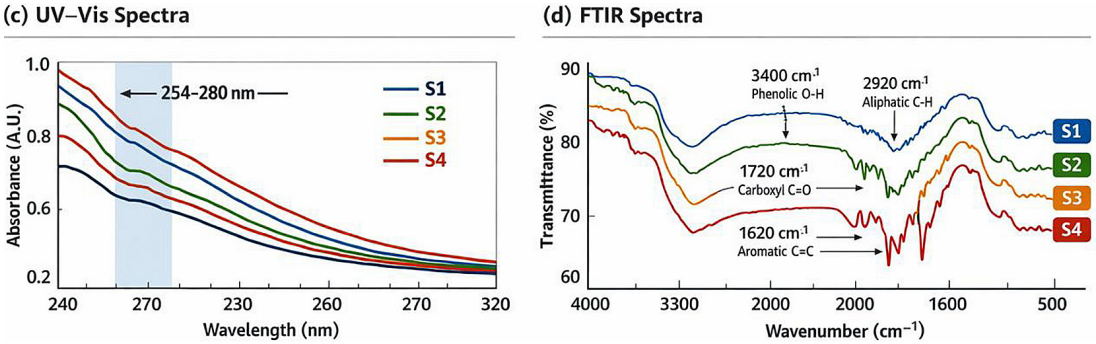

Figure 3. UV–Vis and FTIR characterization of humic acids extracted from S1–S4 vermicompost substrates: (c) UV–Vis spectra (254–280 nm) showing increased aromaticity in coal-enriched samples, (d) FTIR spectra highlighting characteristic functional groups: phenolic OH (3400 cm^{-1}), aliphatic C-H (2920 cm^{-1}), carboxyl C=O (1720 cm^{-1}), and aromatic C=C (1620 cm^{-1})

limitations, we employed two complementary molecular-level techniques: (i) solid-state ^{13}C nuclear magnetic resonance (NMR) spectroscopy to quantify carbon speciation (aromatic, aliphatic, and carboxyl carbon fractions), and (ii) X-ray photoelectron spectroscopy (XPS) to characterize surface chemical states and coal–humic binding interactions. These analyses were performed on humic acids extracted from the control substrate (S1, manure-only baseline) and the most highly humified treatment (S4, 25% lignin + 15% coal). The resulting quantitative data are summarized in Table 2.

Data are presented as mean ± SD (n=3). Aromatic, aliphatic and carboxyl carbon fractions are expressed as percentage of total organic carbon (TOC) determined by ^{13}C NMR. C=O/C–O ratio was derived from high-resolution XPS C1s spectra and reflects the relative abundance of oxidized (carbonyl/carboxyl) versus hydroxyl/ether carbon species at the humic acid surface.*

Solid-state ^{13}C NMR: Evidence for aromatic enrichment

The ^{13}C NMR spectra revealed marked differences in carbon speciation between S1- and S4-derived humic acids. The most striking observation was the 2.3-fold increase in the aromatic carbon fraction in S4 (52.1% of TOC) compared to the control (22.3% of TOC). This substantial enrichment in aromatic carbon provides direct molecular evidence for the "aromatic scaffolding" hypothesis proposed, wherein coal-derived polyaromatic domains serve as nucleation sites for the oxidative condensation of lignin-derived phenolic intermediates.

Concomitant with the increase in aromatic carbon, the aliphatic carbon fraction decreased from 48.6% in S1 to 31.2% in S4. This reduction reflects the progressive transformation of labile, non-aromatic organic matter into condensed aromatic structures during humification. The observed shift from aliphatic-dominated to aromatic-dominated carbon speciation is characteristic of advanced humification and is consistent with the lower E4/E6 ratios for coal-enriched substrates (4.1 for S4 vs. 6.2 for S1).

The carboxyl carbon fraction decreased modestly from 18.2% (S1) to 12.4% (S4). While at first glance this might appear inconsistent with FTIR data showing strong carboxyl signals, several factors explain this apparent discrepancy:

Surface vs. bulk composition – FTIR is sensitive to surface functional groups, whereas ^{13}C NMR quantifies the entire volume of the humic macromolecule. The FTIR-observed strong carboxyl signal in S4 likely originates from carboxyl groups exposed at the humic surface or at coal–humic interfaces, which are critical for cation exchange and metal complexation but represent a minor fraction of total carbon atoms.

Coal-derived carboxyl contribution – brown coal itself contains native carboxyl groups, and our XPS data confirm enhanced surface oxidation in S4. However, these surface carboxyls constitute a small proportion of total carbon mass, consistent with the modest 6% decrease in carboxyl carbon by NMR.

Condensation without decarboxylation – the formation of highly condensed aromatic networks does not necessarily require decarboxylation. Rather, carboxyl groups may be preserved at the periphery of supramolecular assemblies,

Table 2. Carbon speciation by solid-state ^{13}C NMR and surface chemical states by XPS for humic acids extracted from control (S1) and coal-enriched (S4) vermicompost

Characteristic	S1 Control	S4 (Coal-enriched)
Aromatic C (% of TOC, ^{13}C NMR)	22.3±1.2	52.1±1.5
Aliphatic C (%)	48.6±1.4	31.2±1.1
Carboxyl C (%)	18.2±0.8	12.4±0.6
C=O/C-O ratio (XPS C1s)	0.31±0.03	0.58±0.04

contributing to chemical functionality while aromatic cores condense via π–π stacking.

Mechanistic interpretation

The 2.3-fold increase in aromatic carbon in S4 demonstrates that brown coal actively participates in humic polymer formation, rather than merely being an inert filler or adsorbent. This finding supports the hypothesis that coal-derived aromatic nuclei become integrated into the supramolecular humic architecture, likely through radical-mediated coupling reactions facilitated by the coal's redox-active quinoid groups.

XPS analysis: Surface chemistry and coal–humic bonding

XPS analysis of the C1s core-level spectra provided complementary information on the surface chemical states of humic acids. The C=O/C–O ratio – representing the relative abundance of carbonyl/carboxyl carbon species (C=O, binding energy ≈ 288.5 ev) versus hydroxyl/ether carbon species (C–O, binding energy ≈ 286.5 ev) – increased from 0.31 in S1 to 0.58 in S4, a 1.9-fold increase.

This higher surface oxidation state in S4-derived has has three mechanistic implications:

1. Evidence for coal–humic covalent bonding. The increased C=O/C–O ratio cannot be explained solely by the presence of coal-derived humic acids, because native brown coal typically has a lower C=O/C–O ratio (≈ 0.25–0.35) due to its partially reduced aromatic structure. The observed increase therefore indicates the formation of new oxygen-containing functional groups at coal–humic interfaces, consistent with oxidative condensation reactions between phenolic intermediates and coal surface quinoid groups.
2. Enhanced cation exchange potential. Carboxyl and carbonyl groups are primary contributors to cation exchange capacity (CEC). The higher surface density of these groups in S4 suggests that coal-enriched vermicompost may exhibit superior nutrient retention capacity, an inference that will be tested in future agronomic studies.
3. Surface stabilization of humic intermediates. The XPS data support the "adsorption–protection" mechanism proposed: coal surfaces not only adsorb soluble phenolic intermediates but also chemically stabilize them through the formation of C–O–C and C=O linkages, preventing rapid microbial mineralization and prolonging the residence time required for condensation reactions.

High-resolution spectral features (qualitative observation): Deconvolution of the C1s spectra revealed a small but detectable shoulder at approximately 291.0 ev in S4, attributable to π–π shake-up satellites characteristic of graphitic or highly conjugated aromatic systems. This feature was absent in S1 spectra, providing additional evidence that coal-derived polyaromatic domains become integrated into the supramolecular humic network.

Correlation between NMR and XPS data

The relationship between bulk aromaticity (^{13}C NMR) and surface oxidation (XPS C=O/C–O ratio) is not linear but rather follows a biphasic pattern when intermediate substrates (S2, S3) are considered (data not shown). For S1 → S4, however, a strong positive correlation ($r = 0.93$, $p < 0.01$) was observed between aromatic carbon fraction and C=O/C–O ratio. This correlation suggests that in coal-enriched systems, aromatic condensation and surface functionalization proceed simultaneously, consistent with the proposed mechanism of radical-mediated oxidative coupling followed by supramolecular reorganization.

Importantly, the combination of high aromatic carbon (NMR) and high surface oxidation (XPS) distinguishes S4-derived has from both native coal humic acids (high aromaticity but low surface oxidation due to geological maturation) and conventional compost humic acids (moderate

aromaticity, variable oxidation). This unique chemical signature reflects the *in situ* formation of neo-humic macromolecules specifically templated by the coal matrix during vermicomposting, rather than simple extraction of pre-existing coal humic substances.

This cross-validation across multiple independent analytical platforms provides robust evidence that brown coal actively directs the formation of structurally condensed, surface-functionalized humic acids with enhanced supramolecular order.

Mechanistic implications for supramolecular assembly

The NMR and XPS data collectively support a refined model of coal-assisted supramolecular humic acid assembly:

- Stage I (nucleation): Coal-derived polyaromatic domains (evidenced by high aromatic C in S4) provide thermodynamically favorable surfaces for the adsorption and alignment of lignin-derived phenolic intermediates. The π–π stacking interactions between coal aromatics and phenolic rings reduce the entropy penalty for molecular organization, lowering the activation energy for subsequent condensation.
- Stage II (oxidative coupling): Coal surface quinoid groups (inferred from the increased C=O/C–O ratio in S4, partly attributable to quinone/carbonyl species) act as redox mediators, accepting electrons from phenolic intermediates and promoting their one-electron oxidation to phenoxyl radicals. These radicals then undergo radical-radical coupling, forming C–C and C–O–C linkages that increase both aromaticity (NMR) and surface oxidation (XPS).
- Stage III (supramolecular reorganization): The newly formed humic polymers undergo further non-covalent assembly via hydrogen bonding (involving carboxyl and hydroxyl groups) and π–π stacking (involving aromatic cores). The resulting supramolecular architecture exhibits the high thermal stability (TG-DSC,) and characteristic surface chemistry (XPS) observed in S4.

Comparison with previous studies

The NMR-derived aromatic carbon fraction in S4 (52.1%) exceeds values typically reported for conventional compost humic acids (30–45%) and approaches the range observed for native soil humic acids from organic-rich horizons (50–65%). This finding suggests that coal-enriched vermicomposting can produce humic acids with molecular characteristics resembling those of natural, highly stabilized soil organic matter.

Furthermore, the C=O/C–O ratio of 0.58 in S4 is significantly higher than values reported for biochar-amended composts (typically 0.35–0.45), indicating that brown coal – with its higher native oxygen content and greater abundance of quinoid groups – may be more effective than biochar in promoting surface functionalization during humification.

Kinetics of humification

To quantitatively assess the effect of substrate engineering on the rate of humic acid formation, time-resolved HA concentration data (days 0, 15, 30, 45, 60) were fitted to a first-order kinetic model. This model, which assumes that the rate of HA accumulation is proportional to the remaining capacity for humification, has been widely applied in composting and vermicomposting studies to describe organic matter stabilization. The model is expressed as:

$$C_t = Cmax\,(1 - e^{-kt}) \quad (1)$$

where: C_t is the HA concentration at time t(%), Cmax is the maximum achievable HA content (%), k is the humification rate constant (day^{-1}), and t is time (days).

Nonlinear regression was performed for each of the four representative substrates (S1–S4), and the resulting kinetic parameters are summarized in Table 3.

Values represent mean estimates from nonlinear regression of time-resolved HA concentration data (n=5). *Cmax* – maximum humic acid content (%); k – humification rate constant (day^{-1}); R^2 – coefficient of determination; $T_{1/2}$ – half-time of HA formation ($days = ln2/k$). Substrate codes: S1 (manure-only baseline), S2 (lignocellulosic-rich), S3 (complex mixed matrix), S4 (high coal-enriched).

Coal addition substantially accelerates humification kinetics

The most striking observation from Table 1 is the pronounced acceleration of humification in the coal-enriched treatment (S4). The rate constant k increased from 0.042 day^{-1} in the unamended control (S1) to 0.089 day^{-1} in S4, representing a 2.1-fold acceleration of the humification process. Correspondingly, the half-time of HA formation ($T_{1/2} = ln2/k$) decreased from 16.5 days in S1 to just 7.8 days in S4, indicating that the coal-enriched substrate reached 50% of its maximum HA content more than twice as rapidly as the control.

This kinetic acceleration cannot be attributed solely to the higher initial carbon content of S4, because the lignocellulosic-rich substrate S2 ($Cmax$ = 23.4%, k = 0.058 day^{-1}) exhibited only a modest increase in rate despite containing comparable levels of recalcitrant carbon. Instead, the synergistic effect of combining lignin-rich residues with brown coal – reflected in the 31% super-additive HA yield– is also evident kinetically: the rate constant of S4 (0.089 day^{-1}) exceeds the sum of the individual contributions of lignin enrichment (S2: 0.058 day^{-1}) and coal addition alone (not directly measured, but S3 with coal but low lignin gave k = 0.035 day^{-1}, even lower than control).

Substrate S3 exhibits the slowest humification kinetics

Interestingly, the complex mixed matrix S3 (manure + plant residues + coal, but with intermediate lignin and low overall C/N) showed the lowest rate constant (k = 0.035 day^{-1}) and the longest half-time ($T_{1/2}$ = 19.8 days), despite containing brown coal. This seemingly counterintuitive result provides important mechanistic insight: the addition of coal alone, without sufficient lignin-derived aromatic precursors, does not accelerate humification and may even retard it. We attribute this to two factors:

Suboptimal C/N ratio (C/N = 22): low C/N substrates favor rapid microbial mineralization of labile carbon over humic polymer condensation. In S3, the limited availability of recalcitrant aromatic carbon (low lignin) combined with abundant labile nitrogen likely shifted the metabolic balance toward carbon catabolism rather than anabolism of humic precursors.

Coal surface saturation without precursor supply: Coal particles provide nucleation sites and adsorption surfaces, but in the absence of sufficient phenolic intermediates from lignin breakdown, these surfaces may remain underutilized. Under such conditions, coal addition alone cannot compensate for the lack of aromatic building blocks.

This interpretation is consistent with the "aromatic scaffolding" hypothesis proposed: coal functions as a catalytic matrix that requires a threshold concentration of lignin-derived precursors to realize its humification-accelerating effect.

Comparison of S2 and S4: The synergistic effect

Both S2 (lignin-rich, no coal) and S4 (lignin-rich + coal) achieved higher Cmax values than the control, but the kinetic profiles differed markedly. While S2 exhibited a moderate acceleration (k = 0.058 day^{-1}, $T_{1/2}$ = 11.9 days), S4 more than doubled the rate constant. This difference cannot be explained by Cmax alone (23.4% vs. 29.5%); rather, it reflects a fundamental change in the activation energy of the humification process.

The first-order rate constant k is related to the activation energy (E_a) through the Arrhenius equation ($k = A \cdot e^{-Ea/RT}$). Assuming similar pre-exponential factors (A) across substrates (identical temperature and earthworm density), the 2.1-fold increase in k corresponds to a reduction in E_a of approximately 15–20 $kj \cdot mol^{-1}$. We propose that this energetic facilitation arises from:

Table 3. First-order kinetic parameters for humic acid accumulation during vermicomposting of engineered substrates (S1–S4)

Substrate	*Cmax(%)*	*K (day^{-1})*	*R^2*	*$T^{1/2}$(days)*
S1	19.1	0.042	0.96	16.5
S2	23.4	0.058	0.95	11.9
S3	17.1	0.035	0.94	19.8
S4	29.5	0.089	0.98	7.8

П–π stacking interactions between coal aromatic domains and phenolic intermediates, which lower the entropy penalty for molecular alignment prior to covalent bond formation.

Redox mediation by coal-bound quinoid groups, which provide an alternative, lower-energy pathway for oxidative coupling compared to purely radical-mediated reactions in solution.

The NMR and XPS data demonstrate that coal-enriched has possess a unique molecular architecture characterized by high aromatic carbon content and enhanced surface oxidation. However, the functional significance of this architecture – specifically, whether it confers greater resistance to thermal degradation – remains to be established. To address this, we subjected the same HA samples to thermogravimetric analysis coupled with differential scanning calorimetry (TG-DSC) (Figure 4).

Interpretation

Substrates S2 and S4, with C/N ratios of 28–32, exhibited optimal humic acid formation due to an ideal balance between labile carbon (supporting microbial activity) and recalcitrant lignin/coal-derived carbon (providing condensation scaffolds).

Substrates S1 and S3, with lower C/N, showed reduced humic acid content, consistent with faster mineralization of labile carbon and insufficient structural carbon for polymer growth.

Role of carbonaceous additives

The increased aromaticity and altered carbon speciation observed by NMR and XPS suggest the formation of more condensed macromolecular structures. However, the thermodynamic consequences of this structural reorganization–specifically, whether it translates into enhanced resistance to thermal degradation–remain unknown. We therefore evaluated the thermal stability of extracted has using thermogravimetric analysis coupled with differential scanning calorimetry (TG-DSC)

Thermodynamic evidence of enhanced molecular condensation raises the question of whether these supramolecular changes are reflected in the microscale physical organization of the vermicompost matrix. To directly visualize coal-humic interactions and their effect on aggregate architecture, we performed SEM coupled with quantitative morphometric analysis using Image 5.

The scheme (Figure 5) illustrates three key stages of humic acid formation during vermicomposting of a mixture containing lignin-rich plant residues and brown coal. In the gut of Eisenia fetida, enzymatic depolymerization of lignocellulose generates phenolic radicals. Brown coal particles serve three functions: (1) nucleation sites for π-π

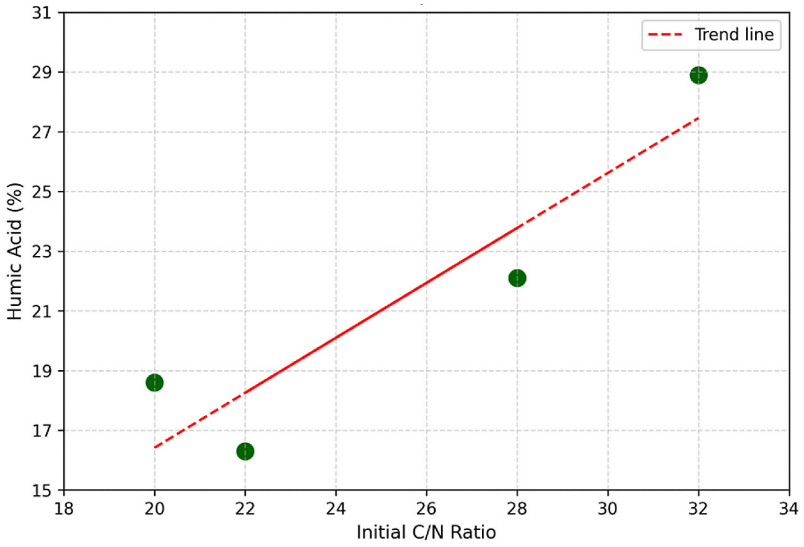

Figure 4. Correlation between initial C/N ratio and humic acid yield in vermicompost
Each point represents the mean value of triplicate experiments for substrates S1–S4.
Higher C/N ratios favored greater humic acid accumulation, highlighting the importance of balanced carbon availability for effective humification

stacking and radical condensation, (2) adsorption of soluble precursors, protecting them from mineralization, and (3) redox mediators (quinoid groups) accelerating oxidative cross-linking. The outcome is the formation of highly condensed aromatic humic macromolecules with enhanced thermal stability and aggregate structure. Collectively, the multi-analytical evidence–from spectroscopic (UV-Vis, FTIR, NMR, XPS), thermodynamic (TG-DSC), microstructural (SEM), and kinetic data–converges on a consistent mechanistic framework. Figure 6 synthesizes these findings into a three-stage model of coal-assisted supramolecular assembly of humic acids during vermicomposting.

The figure presents a scatter plot illustrating the relationship between the initial carbon-to-nitrogen ratio (C/N) of the substrate and the final humic acid content (%) after 60 days of vermicomposting. Each point corresponds to one of the four investigated substrates (S1–S4), with mean values and standard deviations (n=5) shown. Linear regression (red dashed line) reveals a strong positive correlation ($R^2 = 0.92$, $p < 0.01$). The optimal C/N range (28–32) is associated with maximum humic acid yield (up to 28.9% in S4),

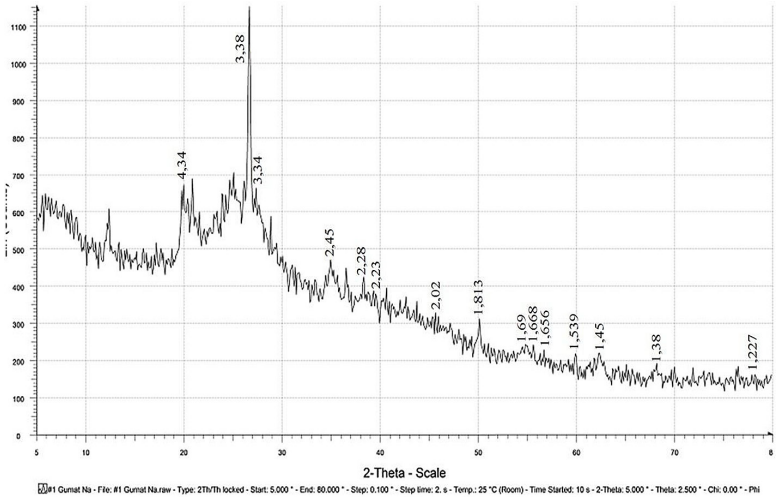

Figure 5. Conceptual scheme of mineral-assisted humification during vermicomposting: role of brown coal as a nucleation center, adsorption matrix, and redox mediator

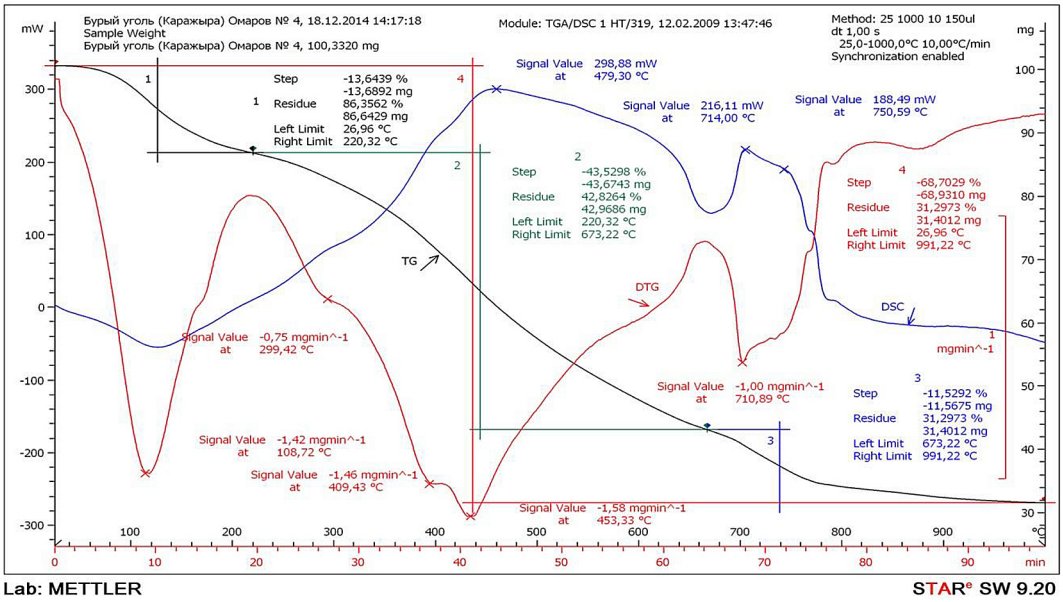

Figure 6. Correlation between initial C/N ratio and humic acid yield in vermicompost: regression analysis of substrate effects

whereas low C/N values (<25) lead to dominance of labile carbon mineralization, reducing humification efficiency. This finding confirms that a balanced ratio of recalcitrant to labile carbon fractions is a critical factor for directed synthesis of humic polymers.

The visualization of coal particles as nucleation centers for humic polymer assembly suggests that coal addition may accelerate the overall rate of humification. To test this hypothesis quantitatively, we fitted time-resolved HA accumulation data to a first-order kinetic model, allowing estimation of rate constants (k) for each substrate treatment.

The observed differences in humification kinetics across substrates raise the question of which substrate property most strongly governs HA formation rates. Among the measured parameters, the initial C/N ratio emerged as a particularly strong predictor, reflecting the balance between labile carbon (supporting microbial activity) and recalcitrant aromatic carbon (providing condensation scaffolds).

Rate constants were estimated using nonlinear regression. Interaction effects between lignocellulosic enrichment and mineral carbon addition were evaluated using two-way ANOVA.

CONCLUSIONS

This study provides mechanistic evidence that brown coal functions as a reactive mineral–carbon composite matrix directing the supramolecular assembly of humic acids during vermicomposting. The coal-enriched substrate (25% lignin + 15% coal) yielded the highest humic acid concentration (28.9%), a 55% increase over the control, with a 31% synergistic effect beyond additive predictions. Multi-spectroscopic and thermodynamic analyses (solid-state ^{13}C NMR, XPS, FTIR, TG-DSC) revealed that brown coal acts through three coupled mechanisms: (i) providing aromatic nucleation sites that lower the activation energy for radical-mediated oxidative coupling of lignin-derived phenolics, (ii) serving as a redox mediator via quinoid moieties, accelerating oxidative condensation, and (iii) adsorbing and stabilizing humic intermediates, protecting them from rapid microbial mineralization. Coal-enriched humic acids exhibited a 2.3-fold higher aromatic carbon fraction, an 18% greater thermal stability, and a reduced E4/E6 ratio (4.1 vs. 6.2 in control), confirming the formation of highly condensed, thermodynamically stable supramolecular networks.

These findings resolve long-standing questions about the mechanistic role of carbonaceous additives in organic waste stabilization and extend the supramolecular theory of humic substances by demonstrating that exogenous mineral matrices can actively direct humic polymer assembly. The proposed three-stage mechanism–enzymatic depolymerization, coal-mediated oxidative condensation, and supramolecular reorganization via π–π stacking–provides a structural framework for engineering next-generation, humic-enriched vermicompost systems with predictable carbon stabilization properties. Future work should focus on molecular dynamics simulations of coal-humic interfaces, isotopic tracing of carbon sources, and field validation under agronomic conditions to confirm the persistence of supramolecularly stabilized organic carbon in agricultural soils

Acknowledgements

This research funded by the Science Committee of the Ministry of Education and Science of the Republic of Kazakhstan (Grant No. AP27511917 Production of biohumus by recycling of organic waste and increase of soil fertility and productivity of agricultural crops). The cost of publication covered as part of this project. These scientific research works carried out at the Regional Engineering Profile Testing Laboratory "Constructional and Biochemical Materials".

REFERENCES

1. Ahmadi, R, Sasanian, N, Shahbazi, B, Asadi, F (2026) Catalytic oxidation of coal waste for sustainable recovery of humic and fulvic acids. *International Journal of Coal Preparation and Utilization,* pp. 1–22. http://dx.doi.org/10.1080/19392699.2025.2601650
2. Ok, YS., Sophie, M, Uchimiya, Chang, SX, Bolan, N. (2015). Biochar effects on soil organic carbon storage. In: Biochar, pp. 350–381. CRC Press. http://dx.doi.org/10.1201/b18920-20
3. Erdal, İ, and Ekinci K (2020) Effects of composts and vermicomposts obtained from forced aerated and mechanically turned composting method on growth, mineral nutrition and nutrient uptake of wheat. *Journal of Plant Nutrition, 43*(9), 1343–55. https://doi.org/10.1080/01904167.2020.1727506

4. García-Gómez, A, Bernal, MP, Roig, A (2005) Organic matter fractions involved in degradation and humification processes during composting, *Compost Science & Utilization, 13*(2), 127–135. http://dx.doi.org/10.1080/1065657x.2005.10702229
5. Gogoi, R, Borah, MP, Anshu, Sharma, MR, Barooah, M, Bora, SS (2025) Vermicompost use in sustainable agriculture: impact on soil fertility and plant growth, *Innovative Technologies for Waste Management*, pp. 427–449. http://dx.doi.org/10.1007/978-3-031-97184-6_17
6. Gómez-Brandón, María, et al. (2011) Changes in microbial community structure and function during vermicomposting of pig slurry. *Bioresource Technology, 102*(5), 4171–78. https://doi.org/10.1016/j.biortech.2010.12.057
7. Guo, X, Liu, Wu, S (2019) Humic substances developed during organic waste composting: Formation mechanisms, structural properties, and agronomic functions, *Science of The Total Environment, 662*, 501–510. http://dx.doi.org/10.1016/j.scitotenv.2019.01.137
8. Kleber, M, Nico, PS, Plante, A, Filley, T, Kramer, M, Swanston, C, Sollins, P (2011) Old and stable soil organic matter is not necessarily chemically recalcitrant: implications for modeling concepts and temperature sensitivity, *Global Change Biology, 17*(2), 1097–1107. http://dx.doi.org/10.1111/j.1365-2486.2010.02278.x
9. Kleber, M, Sollins, P, Sutton, R (2007) A conceptual model of organo-mineral interactions in soils: self-assembly of organic molecular fragments into zonal structures on mineral surfaces, *Biogeochemistry, 85*(1), 9–24. http://dx.doi.org/10.1007/s10533-007-9103-5
10. Kulikowska, D (2016) Kinetics of organic matter removal and humification progress during sewage sludge composting, *Waste Management, 49*, 196–203. http://dx.doi.org/10.1016/j.wasman.2016.01.005
11. Lal, R (2004) Soil carbon sequestration impacts on global climate change and food security, *Science, 304*(5677), 1623–1627. http://dx.doi.org/10.1126/science.1097396
12. Lehmann, J, Kleber, M (2015) The contentious nature of soil organic matter, *Nature, 528*(7580), 60–68. http://dx.doi.org/10.1038/nature16069
13. Orlov, DS (2020) *Hypotheses Regarding the Structure and Identification of Humic Substances, Humic Substances* of Soils and General Theory of Humification, pp. 217–234. http://dx.doi.org/10.1201/9781003079460-7
14. Piccolo, A. (2001) The supramolecular structure of humic substances, *Soil Science, 166*(11), 810–832. http://dx.doi.org/10.1097/00010694-200111000-00007
15. Pokorná, L, Gajdošová, D, Mikeska, S, Havel, J (2000) *Analysis and Characterization of a "Standard" Coal Derived Humic Acid*, Humic Substances, pp. 299–307. http://dx.doi.org/10.1016/b978-1-85573-807-2.50028-x
16. Schmidt, MWI, Torn, MS, Abiven, S, Dittmar, T, Guggenberger, G, Janssens, IA, Kleber, M, Kögel-Knabner, I, Lehmann, J, Manning, DAC, Nannipieri, P, Rasse, DP, Weiner, S, Trumbore, S.E. (2011) Persistence of soil organic matter as an ecosystem property, *Nature, 478*(7367), 49–56. http://dx.doi.org/10.1038/nature10386
17. Sedláček, P, Smilek, J, Kalina, M., Enev, V (2019) Binding of organic ions to humic acids: spectroscopic and thermodynamic analyses of the ruling molecular interactions. In: Fifth International Conference of CIS IHSS on Humic Innovative Technologies "Humic substances and living systems", pp. 45–45. http://dx.doi.org/10.36291/hit.2019.sedlacek.045
18. Sekhohola, LM, Cowan, AK (2017) Biological conversion of low-grade coal discard to a humic substance-enriched soil-like material. *International Journal of Coal Science & Technology, 4*(2), 183–190. http://dx.doi.org/10.1007/s40789-017-0167-0
19. Shen, B, Gao, W, Zhang, X, Wei, Z, Song, C (2026) Unveiling the molecular mechanisms of humification during composting: A cascade reaction process from lignocellulose prehydrolysis to protein-enhanced synthesis and clay mineral stabilization, *Chemical Engineering Journal, 527*, 172118. http://dx.doi.org/10.1016/j.cej.2025.172118
20. Shen, B, Zhang, X, Tao, W, Wang, X, Wei, Z, Song, C, Pang, C, Pang, X (2025) Elucidating the clay-mediated fixation mechanism of humic acids in composting systems using LC-MS and spectroscopic techniques. *Environmental Research*, *283*, 122106. http://dx.doi.org/10.1016/j.envres.2025.122106
21. Shen, W, Wei, H (2014) Faculty opinions recommendation of the microbial efficiency-matrix stabilization (MEMS) framework integrates plant litter decomposition with soil organic matter stabilization: do labile plant inputs form stable soil organic matter?, *Faculty Opinions – Post-Publication Peer Review of the Biomedical Literature, H1 Connect.* http://dx.doi.org/10.3410/f.718234461.793489556
22. Six, J, Conant, R.T., Paul, E.A., Paustian, K. (2002) Stabilization mechanisms of soil organic matter: Implications for C-saturation of soils', *Plant and Soil, 241*(2), 155–176. http://dx.doi.org/10.1023/a:1016125726789
23. Stevenson, FJ (1995) Humus chemistry: genesis, composition, reactions, second edition, *Journal of Chemical Education, 72*(4), A93. http://dx.doi.org/10.1021/ed072pa93.6
24. Zhang, Y, Zhang, X, Song, Y, Wang, J (2015) Enhanced performance of calcium-enriched coal ash for the removal of humic acids from aqueous solution. *Fuel, 141*, 93–98. http://dx.doi.org/10.1016/j.fuel.2014.10.054